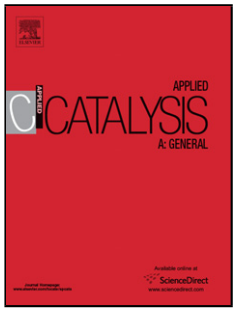

Title: Highly Robust Magnetically Recoverable Ag/Fe_2O_3 Nanocatalyst for Chemoselective Hydrogenation of Nitroarenes in Water

Authors: Astam K. Patra, Nhat Tri Vo, Dukjoon Kim

PII: S0926-860X(17)30096-0
DOI: http://dx.doi.org/doi:10.1016/j.apcata.2017.03.007
Reference: APCATA 16166

To appear in: *Applied Catalysis A: General*

Received date: 13-1-2017
Revised date: 20-2-2017
Accepted date: 7-3-2017

Please cite this article as: Astam K.Patra, Nhat Tri Vo, Dukjoon Kim, Highly Robust Magnetically Recoverable Ag/Fe2O3 Nanocatalyst for Chemoselective Hydrogenation of Nitroarenes in Water, Applied Catalysis A, General http://dx.doi.org/10.1016/j.apcata.2017.03.007

Highly Robust Magnetically Recoverable Ag/Fe_2O_3 Nanocatalyst for Chemoselective Hydrogenation of Nitroarenes in Water

Astam K. Patra, Nhat Tri Vo and Dukjoon Kim*

School of Chemical Engineering, Sungkyunkwan University, Suwon, Gyeonggi 16419, Republic of Korea

Corresponding Author

*Tel.: +82-31-290-7250. Fax: +82-31-290-7270. E-mail: djkim@skku.edu (D.K.).

Graphical abstract

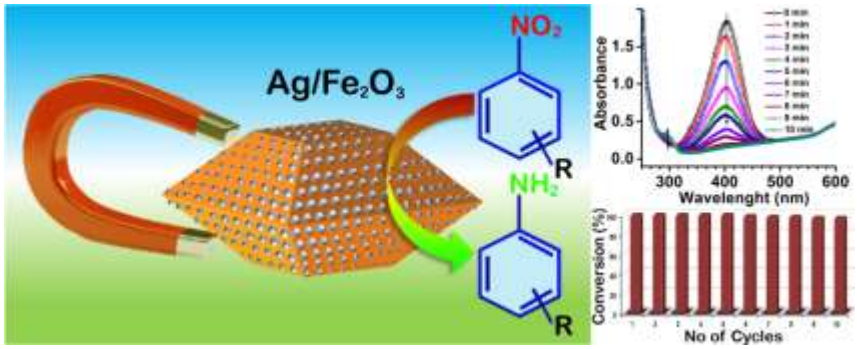

Highlight

- Highly efficient Ag nanoparticles incorporated magnetic α-Fe_2O_3 nanocatalyst were developed by simple method.
- 4-6 nm Ag nanoparticles on the surface of α-Fe_2O_3 are the active suite for the high catalytic activity.
- LC-MS study suggested that the catalytic reaction pathway is –NO_2, –NHOH, –NH_2 and certainly skips the nitrosoarene intermediate step.
- The nanocatalyst are very efficient in the hydrogenation of nitroarenes tolerating –H, −Br, −I, −OH, −OCH_3, −COOH, and −$CONH_2$ functional groups in water.
- High catalytic activity and excellent recyclability and can be separated by external magnet and no significant loss of catalytic activity after 10 recycles.

Abstract

This work reports on additive-free Ag nanoparticles (4-6 nm) deposition on magnetic α-Fe_2O_3 nanocrystals surface by the slow reduction of $AgNO_3$ with $NaBH_4$ in aqueous medium. The EDS analysis revealed that the new materials contain 3.93 weight % of Ag nanoparticle on the surface of α-Fe_2O_3 which are the active suite for hydrogenation reaction. The Ag/Fe_2O_3 nanocatalysts exhibited good catalytic ability toward chemoselective hydrogenation of nitroarenes in water. LC-MS study suggested that the catalytic reaction pathway is –NO_2, –NHOH, –NH_2 and certainly skips the nitrosoarene intermediate step. The nanocatalysts are very efficient in the hydrogenation of nitroarenes tolerating –H, −Br, −I, −OH, −OCH_3, −COOH and −$CONH_2$ functional groups. The nanocatalysts were separated by external magnet and recycled in aqueous medium which offer environmentally and safe approach to this hydrogenation reaction. The catalyst was tested up to 10 recycles and showed no significant loss of catalytic activity.

Keywords: Ag/Fe_2O_3 nanocatalyst; Heterogeneous catalysis; Hydrogenation; Nitroarene reduction in water; Magnetically recoverable

1. Introduction

Metallic nanoparticle incorporated magnetic iron oxide nanomaterials based catalysts have concerned significant research interest in catalysis due to their easy separation, cost effectiveness, nontoxic behaviour and environmentally safe [1-8]. Hematite (α-Fe_2O_3) have better thermodynamic stability than other different iron oxides under ambient environments [9]. On the other hand, only metal nanocatalysts show high catalytic activity but suffer from several problems, such as separation, leaching and aggregation. So metal nanoparticle incorporated magnetic α-Fe_2O_3 nanomaterials created new vision due to their ease magnetic recovery and recyclability with high catalytic activity [1]. Recent research has demonstrated that small size of Ag nanoparticle have high catalytic activity due to their new nanoscale properties [10]. The Ag nanoparticles incorporated α-Fe_2O_3 nanomaterials have been considered as efficient catalysts to replace conventional homogeneous catalysts, which are normally hampered by separation and recyclability. Furthermore silver nanoparticle draw great attention in catalysis due to plasmonic behavior of nanoscale silver [11, 12], high light adsorption efficiency [13], oxygen reduction property [14], dissociation of H_2 molecule [15] and substrates for surface-enhanced Raman spectroscopy (SERS) [16]. The catalytic activity of silver nanoparticles relies on upon the size, shape, atomic and electronic positioning in the exposed facets of nanoparticles [10,17]. But the controlled synthesis of silver nanoparticles on metal oxide surface by a simple method still remains a challenge to the researchers. In the past decades, researchers have established many synthetic strategies, but most of the process are energy exhaustive, need substantial template removal and formed large particles [18]. Here we demonstrated a simple and eco-friendly method to grow monodisperse Ag nanoparticle on magnetic bitruncated-octahedron shaped α-Fe_2O_3 nanocrystals surface. The size of the Ag nanoparticle (4-6 nm) is governed by the controlled reduction of $AgNO_3$ solution with $NaBH_4$ in aqueous medium without any capping agent.

Nitroarenes compounds have different hazardous effect to the environment and heath. The organic contaminant are mostly used in industry to prepare different pesticides, dyes, and explosives [19, 20]. Some nitroarenes compounds (especially 4-nitrophenol) pollute water and these compounds are a serious threat to the environment and public health due to their highly toxic and carcinogenic in nature [21]. On the other hand aromatic amines are intermediates for the productions of important chemicals in dyes, pharmaceuticals, and agricultural industries [22-24]. Most of the hydrogenation of nitroarenes associated with hazardous solvent, required higher temperature, dangerous hydrogen gas or use of expensive hydride source like silanes, N_2H_2, $LiAlH_4$ or $LiBH_4$ [25-27]. Additionally in many methods, hydrogenation process often ends at an intermediate step forming hydroxylamine, or hydrazine, azoarene etc like side products [28]. Hence performing the hydrogenation of nitroarenes in sustainable method with green solvent like water is challenging [29, 30]. Selective hydrogenation of different nitroarenes and nitrobenzene has drawn much attention in the past decades, involving Ag, Au, Pt, Ru, Ni/C and Co/C catalysts [31-36]. In 2012 Dey et al. used Fe(0) catalyst for selective reduction of nitroarenes in water but after the reaction the catalyst transformed to Fe_3O_4 and further cannot be used [37]. In 2014 Sharma et al. found that vasicine can be used for hydrogenation of nitroarenes in water [38]. Dell'Anna et al. used polymer supported palladium nanocrystals as efficient and recyclable catalyst for the reduction of nitroarenes to anilines under mild conditions in water [39]. Kelly et al. selectively reduced the nitroaromatics in water at room temperature using zinc dust, NH_4Cl and commercially available designer surfactant TPGS-750-M [40]. Recently Feng et al. used recyclable Fe/ppm Pd nanoparticles, PEG-containing designer surfactants and $NaBH_4$ for safe and selective nitrogroup reductions in water at room temperature [41]. Here we synthesized Ag nanoparticle decorated magnetic bitruncated-octahedron shaped α-Fe_2O_3 nanocrystals which show high catalytic hydrogenation of nitroarene in water in presence of $NaBH_4$ as hydrogen source. Furthermore, iron(III) is a

harder Lewis acid, compared to late-transition-metal cations, allowing better interaction with nitrogroup of the nitroarene to facilitie the hydrogenation reaction. It is worth pointing out that $NaBH_4$ is sustainable reducing agent which is mild, efficient and very effective for the reduction of nitroaromatic compounds and after reduction it converted water soluble boric acid. In the absence of catalysts, $NaBH_4$ cannot reduce nitrogroups.

2. Experimental Section

2.1 Synthesis of bitruncated-octahedron shaped α-Fe_2O_3 nanocrystals

Bitruncated-octahedron shaped α-Fe_2O_3 nanocrystals were first synthesized according to the procedure reported in our previous work [9]. In this synthesis process, sodium salicylate (0.8 g) and NaOH (0.2 g) were added in 10 mL of water. Iron(III) nitrate nonahydrate (2.02 g) with 3.0 g of water was gradually added to the above solution. 2M NaOH solution was used to adjust the pH = 8. The following mixture solution was stirred for 3 hrs. Then, this solution was hydrothermally treated at 200 °C for 72 hrs in a Teflon-lined stainless steel autoclave. The resulting material was separated and washed several times with water and ethanol. The material was dried at 25 °C under vacuum. Furthermore, to remove the salicylate molecule, the material was extracted with acid-ethanol solution. The material is denoted as S200-BTO.

2.2 Preparation of Ag/Fe_2O_3 nanomaterials

Ag nanoparticles were deposited on the surface of bitruncated-octahedron shaped α-Fe_2O_3 nanocrystals without any capping agent. In this synthesis, 0.2 g S200-BTO (α-Fe_2O_3) nanocrystal was dispersed in 150 mL water by sonication. Then the solution was putted into ice bath with constant stirring. 20 mL 0.01 M $AgNO_3$ solution was added to the above solution and stirred for 30 min. Then 50 mL 0.002 M $NaBH_4$ solution was added slowly to the above mixture. The resultant mixture was stirred for 3 hrs. Then the reaction mixture removes from ice bath and keeps in room temperature for 12 hrs. The sample was collected by centrifugation

and wash with water and methanol several times. The sample was dry in vacuum in room temperature. The material is denoted as Ag/Fe_2O_3 nanocatalyst.

2.3 Catalysis procedure

In the hydrogenation of nitroarene, the kinetics, effect of solvent, amount of catalyst and amount of $NaBH_4$ were carried out on 4-nitrophenol as model reagent in room temperature. In the typical experiment, 2 ml of 0.1 mmol/L 4-nitrophenol aqueous solution was taken into a 3 mL cuvettes and 500 µL of 1 mg/mL catalyst aqueous solution was added to it. Then 200 µL of 10 mmol/L of $NaBH_4$ aqueous solution was added. The reaction was monitoring by UV-Vis spectrometer at regular intervals of time. The solvent effect, amount of catalyst and amount of $NaBH_4$ was studies in similar reaction condition. The intermediate products of 4-nitrophenol reduction were identified by using a liquid chromatograph-mass spectrometer (Agilent Model 1100 LC-MS ion trap with C18 Column and negative ion mode). Here to decrease the rate of reaction, 20 mL of 0.5 mmol/L 4-nitrophenol aqueous solutions was taken and 1 mL of 1 mg/mL catalyst aqueous solution was added to it. Here we increase the ratio between 4-nitrophenol to catalyst to decrease the rate of reaction. Then 1 mL of 0.1 mmol/mL of $NaBH_4$ aqueous solution was added and the solution was stirred. 10 µL of the aliquot was injected for analysis and acetonitrile–water mixture (30: 70) was used as an eluent with the column temperature at 298 K and 1 mL/ min flow rate. For different nitroarene reduction, 0.2 mmol of nitroarene compound was dispersed in 10 mL water and 5 mg of catalyst was added into a 25 mL sealed tube. The solution was sonicated for 5 min and was placed in an oil bath at 100 °C under vigorous stirring. 2 mmol of $NaBH_4$ was added to the solution and closed the cap and continues reaction. After 30 min of reaction, the magnetic catalyst was recovered by an external magnet and the solution was transferred to 100 mL beaker. Then 20 mL of ethyl acetate was added to it. Then take all the solution in separating funnel and shake it. Then the organic layer was collect and dried over Na_2SO_4 and evaporated to dryness to give the colorless crude

product. The isolated crude product was characterized by ^{1}H (shown in the Supporting Information), respectively.

2.4 Leaching test

To know the true heterogeneous nature of the catalyst, we performed the leaching test. 1 mmol of 4-nitrophenol was dissolve in 10 ml water and 5 mg of catalyst was added to it. The solution was sonicated for 2 min and was placed in an oil bath at 100 °C under vigorous stirring. 2 mmol of $NaBH_4$ was added to the solution and closed the cap and continues reaction. After 8 min, the reaction was stopped and removed all the catalyst from the solution by centrifuging at 10,000 rpm. Then collect the aliquot and continue the reaction for another 10 min.

2.5 Recyclability of the Ag/Fe_2O_3 nanocatalyst

The reusability of the Ag/Fe_2O_3 nanocatalyst was examined for 4-nitrophenol reduction reaction in water. For this reaction, 0.2 mmol of 4-nitrophenol was dissolved in 10 ml water into a 25 mL sealed tube and 5 mg catalyst was added. The solution was sonicated for 2 min and was placed in an oil bath at 100 °C under vigorous stirring. 2 mmol of $NaBH_4$ was added to the solution and closed the cap and continues reaction. After completion of the reaction, the magnetic catalyst was recovered by an external magnet and the solution was decanted. The catalyst was washed thoroughly with ethanol several times. For the next reaction, the catalyst was activated through drying at 100 °C for 3 hrs and used for subsequent recycling experiments. The recycling was performed for ten repetitive reaction cycles.

2.6 Characterization

The Ag/Fe_2O_3 nanocatalyst were examined by different characterization techniques. Purity and crystallinity of the samples were studied by a Bruker D-8 Advance diffractometer operated at 40 kV voltage and 40 mA current using Cu Kα (λ = 0.15406 nm) radiation. HRTEM, EDS and lattice indices images were recorded in a JEOL JEM-2100F TEM operated at 200 kV. FE SEM

(JEOL JEM-7600F) was used for the morphology analysis. Nitrogen sorption analysis were carried out by a Micromeritics Instrument ASAP 2000 surface area analyzer at 77 K. XPS was done on a Thermo Scientific (Model No ESCALAB 250Xi) X-ray Photoelectron Spectrometer operated at 15 kV and 20 mA with a monochromatic Al K_α X-ray source. UV-visible spectra were recorded on a UV/Vis Scanning Spectrophotometer (Beckman Coulter DU 730 Model). The intermediates of 4-nitrophenol reduction were supervised by liquid chromatograph-mass spectrometer (LC-MS, Agilent Model 1100). The hydrogenation products were recognised by Fourier transform-nuclear magnetic resonance spectroscopy (FT-NMR) using a UniyInovq 500 (Varian, U.S.A.) NMR spectrometer. The products were dissolved in DMSO-d_6 before ^{1}H NMR measurement.

3. Results and Discussion

3.1 Ag/Fe_2O_3 Nanocatalyst Synthesis and Structural Study

The synthesis process for Ag nanoparticle decorated bitruncated-octahedron-shaped α-Fe_2O_3 nanocrystal (denoted as Ag/Fe_2O_3) via simple method is shown in Scheme 1. Here we have developed a facile and simple method to prepare Ag/Fe_2O_3 nanocatalyst. Bitruncated-octahedron shaped α-Fe_2O_3 nanocrystals were first synthesized by hydrothermal method according to our previous work [9]. The Ag nanoparticle was deposited on bitruncated-octahedron-shaped α-Fe_2O_3 nanocrystal without any capping agent. Here α-Fe_2O_3 nanocrystal was dispersed in water along with $AgNO_3$ solution and stirred in ice bath. The hydrophilic hydroxyl groups on α-Fe_2O_3 surface can easily coordinate with Ag^+ ions.

The Ag^+ cation was then reduced to Ag(0) slowly by addition of $NaBH_4$ solution following the chemical equation.

$$2NaBH_4 + 2AgNO_3 + 6H_2O = 2Ag + 7H_2 + 2H_3BO_3 + 2NaNO_3$$

But in the presence of Ag nanoparticles in the reaction medium, the reduction rate of the reaction was increased rapidly which increased the crystal growth of Ag. So we used ice bath to control reaction rate and decrease the growth of Ag nanoparticles. In literature several research groups used template molecule to control the size of Ag nanoparticles. But template molecule were cover the surface of Ag nanoparticle and subsequent removal are very dificult and show low catalytic reactivity. Here small size Ag nanoparticle were deposited on the surface of α-Fe_2O_3 with out any template molecule which make it a promissing catalyst. The structural features, crystallinity, and purity of the prepared Ag/Fe_2O_3 nanomaterials were measured, and the achieved XRD pattern is shown in Fig. 1. The X-ray diffraction pattern clearly specified the presence of two phases, i.e. Ag and α-Fe_2O_3; because the obtained XRD pattern matches the JCPDS 04-0783 for cubic Ag metal and JCPDS 01-084-0308 for α-Fe_2O_3 [42,43]. The XRD pattern are indexed according to the 2θ values for silver and iron oxide as shown in Fig. 1. The peaks at 2θ values 24.2, 33.3, 35.7, 41.0, 43.7, 49.7, 54.3, 57.7, 62.7, 64.3 and 64.3° are assigned to (012), (104), (110), (113), (024), (116), (122), (214), and (300) planes of α-Fe_2O_3, respectively [43,44]. The peaks at 2θ values 38.1, 44.3 and 64.5° are assigned to (111), (200) and (220) planes of silver, respectively [42]. This wide angle XRD analysis evidently specifies that the Ag and α-Fe_2O_3 are both highly crystalline in nature.

3.2 Nanostructure and Composition Analysis

Fig. 2 displays the high resolution field-emission scanning electron microscope (FE-SEM) images of S200-BTO and Ag/Fe_2O_3 nanomaterials. FE-SEM images were used to study the size and morphological features of nanomaterials. Fig. 2 clearly indicates that α-Fe_2O_3 nanocrystals are identical in particle size (length: 310 ± 50, width: 220 ± 20, height: 150 ± 10) and Ag nanoparticles were deposited on the surfaces. The images also exhibit that the nanomaterials are well dispersed and moreover, we could clearly see the faces of all the bitruncated-octahedron shaped nanocrystals. High resolution transmission electron microscopy

(HR TEM) was used to investigate the shape, size, and different surfaces of exposed facets of the nanomaterials. The Ag and α-Fe_2O_3 nanocrystals both are clearly seen in Fig. 3a, having the shape of spherical and bitruncated-octahedron respectively.

We found that through the specimen, the Ag nanoparticles had a uniform size of 4-6 nm along with some 25 nm particle. Fig. 3b displays an individual bitruncated-octahedron particle along with Ag nanoparticles. A closer view of the image in Fig. 3b is acquired from the lower side and different Ag nanoparticles are seen more clearly in Fig. 3c. The Fig. 3d is acquired from a closer view of Fig. 3c, and different classes of lattice fringes are resolved. The lattice spacing of the bitruncated-octahedron is 0.25 nm, which agrees to (110) lattice planes in α-Fe_2O_3 crystal [9]. The lattice spacing in the Ag nanoparticles is 0.23 nm, matching to the (111) and equivalent lattice planes of the cubic Ag crystal phase [21]. The TEM images indicated that the Ag nanoparticles with particle sizes less than 10 nm were grew in the surfaces of the bitruncated-octahedron shaped α-Fe_2O_3 nanocrystals with well define nanostructure.

The elemental composition of the prepared Ag/Fe_2O_3 nanomaterials was investigated by elemental mapping and EDS analysis. Fig. 4 shows the elemental mapping and EDS spectrum of Ag/Fe_2O_3 nanomaterials. We recorded a dark-field STEM image (Fig. 4a) and performed elemental mapping for Ag/Fe_2O_3 nanomaterials. Elemental mapping for Fe, O and Ag is shown in Fig. 4b, c, and d respectively, and all the elements are spread over the whole image. Peaks for the elements Fe, O and Ag are clearly seen in the EDX spectrum which revealed that the Ag/Fe_2O_3 nanomaterials is composed of Fe, O and Ag and the elements are present 60.23, 35.84 and 3.93 wt.% respectively.

3.3 XPS and Surface Composition Analysis

XPS analysis was carried out before and after Ag nanoparticles loading on α-Fe_2O_3 nanocrystals surface to examine the oxidation states, surface composition of the elements and

amount of Ag metal present in the Ag/Fe_2O_3 nanomaterials. Fig. 5 displays the XPS results corresponding to the Ag/Fe_2O_3 materials. The binding energy of C 1s line to 284.6 eV is used as reference to correct the binding energies of elements obtained in the XPS analysis [45,46].

The survey XPS profile (Fig. 5a) revealed that the S200-BTO and Ag/Fe_2O_3 nanomaterials are composed of Fe, O and Fe, O, Ag respectively. The elemental composition of Ag/Fe_2O_3 is calculated as (atomic %): Fe 55.62, O 43.26, Ag 1.12. In the high-resolution Fe spectra (Fig. 5b), both materials show two peaks at binding energies of 710.68 eV for Fe $2p_{3/2}$ and 724.36 eV for Fe $2p_{1/2}$. The satellite peaks appear at 718.75 eV binding energy which is characteristic of Fe^{3+} in α-Fe_2O_3 [44]. The deposition of Ag on surface of the particle does not change the oxidation state of Fe significantly. The high-resolution O 1s spectra of S200-BTO (Fig. 5c) show two peaks which are located at 529.3, and 530.9 eV. But O 1s spectra of Ag/Fe_2O_3 show three peaks which are located at 529.3, 530.9 and 531.9 eV. The peaks at 529.3 eV are assigned to the lattice oxygen atoms binding with Fe (Fe–O) and the peaks at 530.9 are assigned to the surface hydroxyl groups (Fe–OH) [47]. The new peak at 531.9 is assigned to Fe-O-Ag (surface complexation) [42]. The high-resolution Ag 3d spectrum (Fig. 5d) show two peaks and these two peaks are located at 367.75 eV for Ag $3d_{5/2}$ and 373.79 eV for Ag $3d_{3/2}$ with a spin–orbit splitting of 6 eV for the Ag $3d_{5/2}$ and Ag $3d_{3/2}$ states which is characteristic of silver metal [48]. The results indicate silver nanocrystals were successfully deposited on the surface of the α-Fe_2O_3 nanocrystals.

3.4 Catalytic Hydrogenation Reaction

The catalytic reactivity of the Ag/Fe_2O_3 nanocatalyst is examined with different nitroarene compounds. Reactivity of the nanocatalyst depends on many factor like surface area, electronic, and atomic structure etc. The BET N_2 sorption method is used to measure the surface area [49-

51]. The BET surface areas for the S200-BTO and Ag/Fe_2O_3 nanocatalysts are determined as 16.3 and 19.58 m^2g^{-1}, respectively. Further the EDS and XPS analysis revealed that the materials contain 3.93 weight % of Ag metal nanoparticles on the surface of α-Fe_2O_3 nanocrystals which are the active suite for hydrogenation reaction using $NaBH_4$. Here we explored the kinetics, effect of solvent, amount of catalyst and amount of $NaBH_4$ in the hydrogenation reaction and 4-nitrophenol was chosen as model reagent in room temperature (25 °C). As seen from Table 1, Ag/Fe_2O_3 nanocatalyst showed high catalytic activity in hydrogenation of 4-nitrophenol to aminophenol by $NaBH_4$ in the water solvent. But in the absence of catalyst, the hydrogenation rate of nitrophenol is very slow.

The hydrogenation reaction also carried out with α-Fe_2O_3 (S200-BTO) but without Ag, α-Fe_2O_3 does not show any activity. From Table 1, we observed that conversions of 99%, 94%, and 8% take place in water, water-ethanol (50/50 in v/v) and ethanol solvent respectively. It was found that organic solvents such as DMF, DCM, THF and acetronitrile almost failed to initiate the reaction, whereas the reduction proceeded efficiently in water. Interestingly the reaction proceeds very slowly in ethanol too. Thus, water has a critical role in this reaction. The hydrogenation of 4-nitrophenol is shown in Fig. 6a. The progress of the hydrogenation reaction was monitored through their UV-vis absorption spectra. 4-nitrophenol in aqueous solution shows absorption maxima around 317 nm. With the addition of sodium borohydride solution, the 4-nitrophenolate ion was formed immediately in the basic medium and the peak has been shifted to around 400 nm. The corresponding final product, 4-aminephenol shows an absorption band around 296 nm. From the UV-Vis spectra, it is clearly seen that a gradual decrease in absorption band around 400 nm is accompanied by simultaneous increase in absorption band around 296 nm which indicates the gradual conversion of 4-nitrophenolate into 4-aminophenol [52]. The two isosbestic points were seen at 277 and 312 nm. It specifies the conversion of 4-nitrophenolate into 4-aminophenol occurred without any side reactions.

Fig. 6b and c show that the conversion was increase with increase the amount of $NaBH_4$ and catalyst. Fig. 6d shows that the catalyst can be separated by external magnet. The evolution of the reaction was monitored by liquid chromatograph-mass spectroscopy. The hydrogenation over Ag/Fe_2O_3 nanocatalyst, major intermediates were recognized by LC-MS and are summarized in Table S1. The intermediates were confirmed by ESI-MS (Fig. S1 and S2). The intermediates were recognized by liquid chromatography (retention time 6.06 min, m/z 138 denoted compound P1; retention time 1.71 min, m/z 214 denoted compound P2; and retention time 1.25 min, m/z 109 denoted compound P3). We observed the formation of –NHOH transient species in the LC-MS spectra of reaction mixture at an intermediate step during monitoring the progress of the reaction. The –NHOH transient species vanishes with time as the reaction proceed.

According to the observations described above, we propose a general mechanistic pathway for the Ag/Fe_2O_3 catalyzed reduction of nitroarenes and shown in Fig. 7. It is suggested that the reaction pathway is $–NO_2$, –NHOH, $–NH_2$. Other product like azoxy-, azo-, or hydrazobenzenes was not detected. Here the B−H bond cleavage occurs on the surface of Ag/Fe_2O_3 nanocatalyst to give the [Ag]-H species (Fig. 7). Such high reactive species are responsible for the rapid reduction of nitroarenes into the corresponding hydroxylamines with very fast reaction kinetics and possibly skips the nitrosoarene intermediate. Fountoulaki et al. also found similar type of mechanistic pathways in reduction of nitroarenes in the presence of supported gold nanoparticle[26]. So the performance of Ag/Fe_2O_3 nanocatalyst depends on so many parameters especially amount of catalyst, solvent, amount of $NaBH_4$ and the substrate concentration. Further we started our study for hydrogenation of different nitrocontaining aromatics at 100 °C because many nitroaromatics does not dissolve in water in room temperature. But solubility of these nitro compounds was increased in water at 100 °C. We

started our study with hydrogenation of 4-nitrophenol (0.2 mmol) in water (10 mL) with the Ag/Fe_2O_3 nanocatalyst (5 mg) in a sealed tube at 100 °C. No catalytic conversion was taking place in the absence of $NaBH_4$. When $NaBH_4$ was added as hydrogen source, the reaction was taking place and conversion reached 99.5% and complete the reaction within 30 min with high selectivity. The turnover frequency for Ag/Fe_2O_3 nanocatalysts was reached 218.5 h^{-1} when the $NaBH_4$/4-nitrophenol molar ratio was 10:1 with 1.821 x 10^{-3} mmol Ag catalyst. Interestingly, it is prominent that Ag/Fe_2O_3 nanocatalysts shows a superior catalytic activity in the reduction of 4-nitrophenol to that of Ag reported in literature (see Table S2). Remarkably, $NaBH_4$ is mild, efficient and very active for the hydrogenation of nitroarenes compounds in water. Because in the presence of Ag metal in the reaction medium, it produces hydrogen gas and water soluble sodium borate following the reaction:

$$NaBH_4 + 2H_2O \rightarrow NaBO_2 + 4H_2$$

$$NaBO_2 + H_2O = H_3BO_3 + NaOH$$

The hydrogen gas reduced the nitro compound to amine and $NaBO_2$ produced water soluble boric acid which can be separated easily. We employed this method several nitroarenes. The results are summarized in Table 2. Interestingly, 4-nitrobenzoic acid was successfully reduced to 4-aminobenzoic, because it is a highly challenging example of such a reduction in the presence of a free carboxylic acid. The hydrogenation of nitroarenes is also proceeds further with other valuable substituents ($CONH_2$, OCH_3, OH, Br, I etc).

The catalyst shows poor catalytic activity for 2-nitrophenyl phenyl ether due solubility problem in water and steric hindrance effect of O-phenoxy group. The α-Fe_2O_3 (S200-BTO) materials does not show any activity in the hydrogenation reaction of nitrophenol in hot water also. To know the true heterogeneous nature of the catalyst we performed the leaching test (see experimental section) [45]. After removal of catalyst no further reaction was taking place. The

reusability of the Ag/Fe_2O_3 nanocatalyst in the hydrogenation reaction was examined using 4-nitrophenol as a reference, and the recycling of the catalyst was conducted for ten repetitive cycles. The results are shown in Fig. 8, suggesting good catalytic efficiency and nanocatalysts did not show significant deactivation during the ten consecutive catalytic runs. In order to check the stability and possibility of leaching, we performed high resolution TEM and powder XRD analyses of the reused catalyst Ag/Fe_2O_3 nanocatalysts. Fig. S3 and S4 suggested that the catalyst structure remain same after the catalytic hydrogenation of nitroarene to corresponding amine compound. From these results, we can conclude that our Ag/Fe_2O_3 nanomaterial is highly efficient in catalysing hydrogenation of nitroarene under mild and eco-friendly reaction conditions.

4. Conclusions

In conclusion, a robust and green protocol has been developed for the hydrogenation of functionalized nitroarenes to the corresponding primary amines. Here Ag/Fe_2O_3 nanocatalyst has been developed by a very simple and an environmentally friendly method. Small particle sizes (4-6 nm) of Ag nanoparticles were successfully deposited on the surface of bitruncated-octahedron shaped α-Fe_2O_3 nanocrystals without any capping agent. Ag/Fe_2O_3 nanocatalyst showed groups in the presence of $NaBH_4$ in the aqueous medium. This new Ag/Fe_2O_3 nanocatalyst show good heterogeneous nature and presence of magnetic α-Fe_2O_3 particle, the recovery of the catalyst can be easily done by external magnet and the catalyst was reused very efficiently. The catalyst shows high TOF value in the reaction. The unique catalytic role played by the Ag/Fe_2O_3 nanocatalyst may contribute significantly in heterogeneous catalyst in green water solvent.

Acknowledgements

DK received grant from the National Research Foundation of Korea, which is funded by the Korean Government (MEST) (NRF-2010-0027955).

Reference

[1] D. Wang, D. Astruc, Chem. Rev. 114 (2014) 6949-6985.

[2] Y. Hou, F. Zuo, A. Dagg, P. Feng, Angew. Chem. Int. Ed. 52 (2013) 1248-1252.

[3] S. De, S. Dutta, A. K. Patra, B. S. Rana, A. K. Sinha, B. Saha, A. Bhaumik, Appl. Cat. A: Gen. 435– 436 (2012) 197– 203

[4] M. Zayat, F. del Monte, M. P. Morales, G. Rosa, H. Guerrero, C. J. Serna, D. Levy, Adv. Mater. 15 (2003) 1809-1812.

[5] K. Narasimharao, A. Al-Shehri, S. Al-Thabaiti, Appl. Cat. A: Gen. 505 (2015) 431–440.

[6] F. Shi, M. K. Tse, M.-M. Pohl, A. Brückner, S. Zhang, M. Beller, Angew. Chem. Int. Ed. 46 (2007) 8866-8868.

[7] C. Fukuhara, K. Hayakawa, Y. Suzuki, W. Kawasaki, R. Watanabe, Appl. Cat. A: Gen. 532 (2017) 12–18

[8] G.V. Mamontov, M.V. Grabchenko, V.I. Sobolev, V.I. Zaikovskii, O.V. Vodyankina, Appl. Cat. A: Gen. 528 (2016) 161–167.

[9] A. K. Patra, S. K. Kundu, A. Bhaumik, D. Kim, Nanoscale 8 (2016) 365-377.

[10] B. Ramaraju, T. Imaea, A. G. Destaye, Appl. Cat. A: Gen. 492 (2015) 184–189.

[11] É. McClean-Ilten, D. Zerulla, Adv. Optical Mater. 4 (2016) 413-418.

[12] K. An, G. A. Somorjai, ChemCatChem 4 (2012) 1512-1524.

[13] P. Wang, B. Huang, X. Zhang, X. Qin, H. Jin, Y. Dai, Z. Wang, J. Wei, J. Zhan, S. Wang, J. Wang, M.-H. Whangbo, Chem. Eur. J. 15 (2009) 1821-1824.

[14] J. H. Lopes, S. Ye, J. T. Gostick, J. E. Barralet, G. Merle, Langmuir 31 (2015) 9718-9727.

[15] A. B. Mohammad, K. Hwa Lim, I. V. Yudanov, K. M. Neyman, N. Rosch, Phys. Chem. Chem. Phys. 9 (2007) 1247-1254.

[16] Z. Lou, Z. Wang, B. Huang, Y. Dai, ChemCatChem 6 (2014) 2456-2476.

[17] T. Benkó, A. Beck, K. Frey, D. F. Srankó, O. Geszti,G. Sáfrán, B. Maróti, Z. Schay, Appl. Cat. A: Gen. 479 (2014) 103–111

[18] E. Skrzynska, S. Zaid, A. Addad, J. S. Girardon, M. Capron, F. Dumeignil, Catal. Sci.Technol. 6 (2016) 3182-3196.

[19] R. S. Wijker, J. Bolotin, S. F. Nishino, J. C. Spain, T. B. Hofstetter, Environ. Sci.Technol. 47 (2013) 6872-6883.

[20] K.-S. Ju, R. E. Parales, Microbiol. Mol. Bio. Rev. 74 (2010) 250-272.

[21] M. Kaloti, A. Kumar, N. K. Navani, Green Chem. 17 (2015) 4786-4799.

[22] A. M. Tafesh, J. Weiguny, Chem. Rev. 96 (1996) 2035-2052.

[23] A. Corma, P. Concepción, P. Serna, Angew. Chem. 119 (2007) 7404-7407.

[24] G. Vilé, D. Baudouin, I. N. Remediakis, C. Copéret, N. López, J. Pérez-Ramírez, ChemCatChem 5 (2013) 3750-3759.

[25] D. Cantillo, M. M. Moghaddam, C. O. Kappe, J. Org. Chem. 78 (2013) 4530-4542.

[26] S. Fountoulaki, V. Daikopoulou, P. L. Gkizis, I. Tamiolakis, G. S. Armatas, I. N. Lykakis, ACS Catal. 4 (2014) 3504-3511.

[27] A. Shukla, R. K. Singha, T. Sasaki, R. Bal, Green Chem. 17 (2015) 785-790.

[28] H. K. Kadam, S. G. Tilve, RSC Adv. 5 (2015) 83391-83407.

[29] Y. Liu, Z. Chen, X. Wang, Y. Liang, X. Yang, and Z. Wang, ACS Sustainable Chem. Eng. 5 (2017) 744-751.

[30] H. Weingärtner, E. U. Franck, Angew. Chem. Int. Ed. 44 (2005) 2672-2692.

[31] Q. Geng and J. Du, RSC Adv. 4 (2014) 16425–16428.

[32] E. Seo, J. Kim, Y. Hong, Y. S. Kim, D. Lee, and B.-S. Kim, J. Phys. Chem. C 117 (2013) 11686-11693.

[33] Y. Xie, N. Xiao, C. Yu, J. Qiu, Catal. Commun. 28 (2012) 69-72.

[34] A. K. Patra, S. K. Kundu, D. Kim, and A. Bhaumik, ChemCatChem 7 (2015) 791 – 798

[35] X. Yang, Y. Liang, Y. Cheng, W. Song, X. Wang, Z. Wang, J. Qiu, Catal. Commun. 47 (2014) 28-31.

[36] P. Zhang, C Yu, X Fan, X Wang, Z Ling, Z. Wang and J. Qiu, Phys. Chem. Chem. Phys., 17 (2015) 145-150.

[37] R. Dey, N. Mukherjee, S. Ahammed, B. C. Ranu, Chem. Commun. 48 (2012) 7982-7984.

[38] S. Sharma, M. Kumar, V. Kumar, N. Kumar, J. Org. Chem. 79 (2014) 9433-9439.

[39] M. M. Dell'Anna, S. Intini, G. Romanazzi, A. Rizzuti, C. Leonelli, F. Piccinni, P. Mastrorilli, J. Mol. Catal. A: Chem. 395 (2014) 307-314.

[40] S. M. Kelly, B. H. Lipshutz, Org. Lett. 16 (2014) 98-101.

[41] J. Feng, S. Handa, F. Gallou, B. H. Lipshutz, Angew. Chem. Int. Ed. 55 (2016) 8979-8983.

[42] D. Li, J. Liu, H. Wang, C. J. Barrow, W. Yang, Chem. Commun. 52 (2016) 10968-10971.

[43] A. K. Patra, A. Dutta, A. Bhaumik, ACS Appl. Mater. Interfaces 4 (2012) 5022-5028.

[44] A. K. Patra, A. Dutta, A. Bhaumik, Chem. Eur. J. 19 (2013) 12388-12395.

[45] N. Pal, E.-B. Cho, A. K. Patra, D. Kim, ChemCatChem 8 (2016) 285-303.

[46] A. K. Patra, A. Dutta, M. Pramanik, M. Nandi, H. Uyama, A. Bhaumik, ChemCatChem 6 (2014) 220-229.

[47] Y. Jia, X.-Y. Yu, T. Luo, M.-Y. Zhang, J.-H. Liu, X.-J. Huang, Dalton Trans. 42 (2013) 1921-1928.

[48] G. Carraro, D. Barreca, A. Gasparotto, C. Maccato, Surf. Sci. Spectra 19 (2012) 1-12.

[49] A. Dutta, M. Pramanik, A. K. Patra, M. Nandi, H. Uyama, A. Bhaumik, Chem. Commun. 48 (2012) 6738-6740.

[50] A. K. Patra, A. Dutta, and A. Bhaumik, J. Phys. Chem. C, 118 (2014) 16703–16709.

[51] V. Kumari, A. K. Patra, A. Bhaumik, RSC Adv. 4 (2014) 13626-13634.

[52] A. K. Patra, A. Dutta, A. Bhaumik, Catal. Commun. 11 (2010) 651-655.

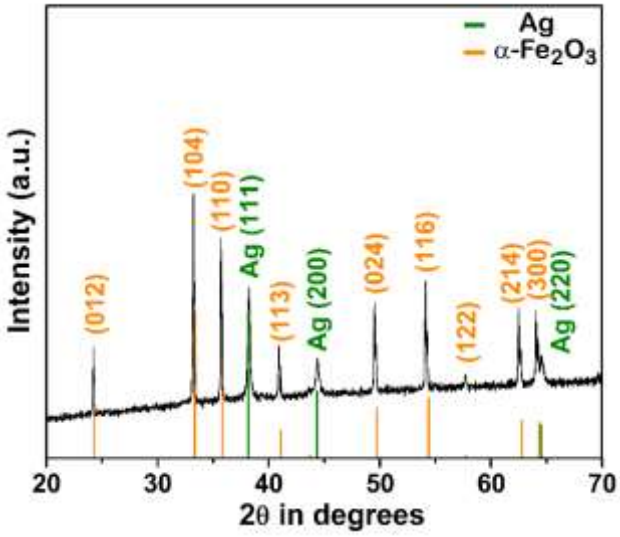

Fig. 1. Wide angle XRD pattern of the highly crystalline Ag/Fe_2O_3 nanocrystals and the peaks are indexed to the α-Fe_2O_3 and cubic Ag phase.

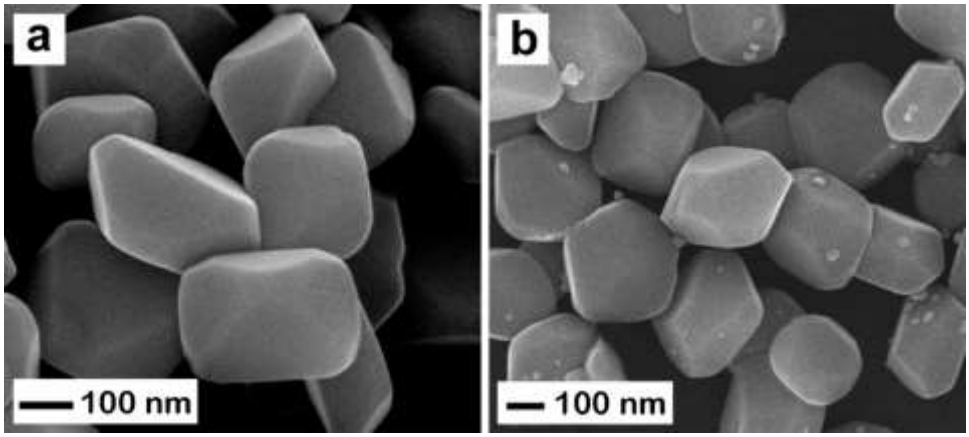

Fig. 2. High resolution FE-SEM images of (a) S200-BTO and (b) Ag/Fe_2O_3 nanomaterials.

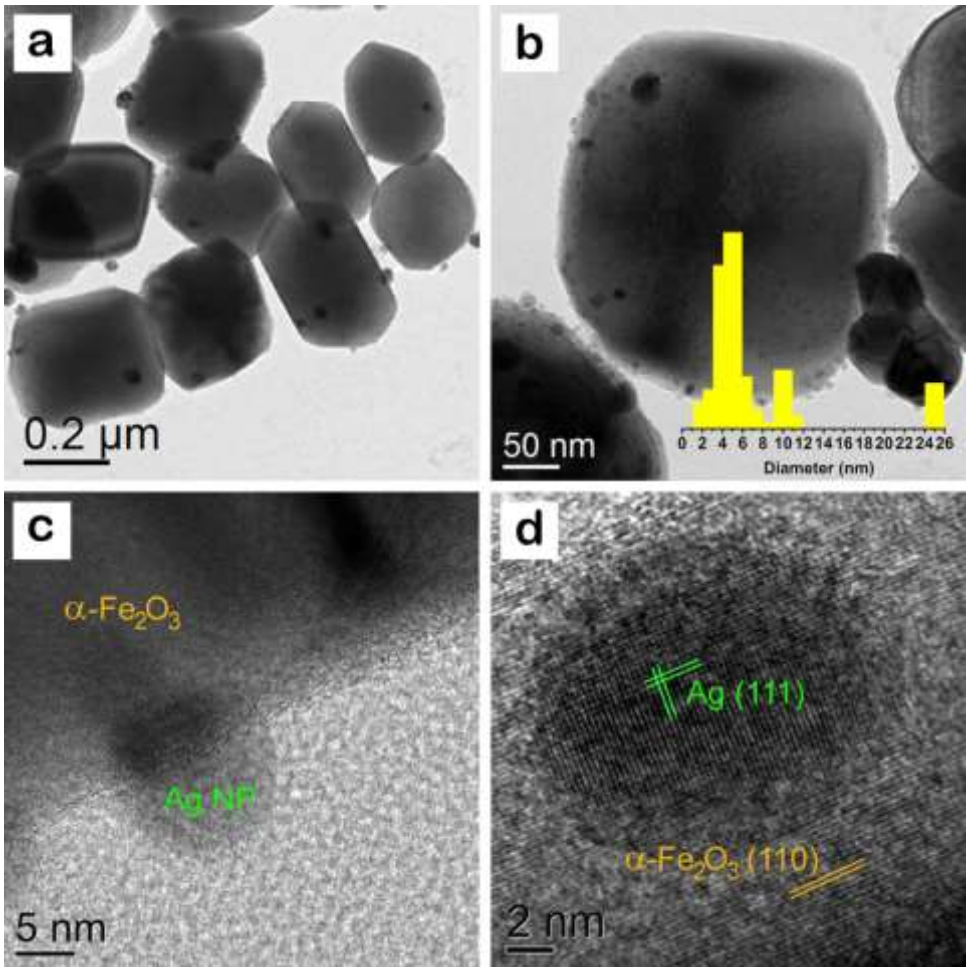

Fig. 3. (a) TEM image of Ag/Fe_2O_3 nanomaterials, (b) HRTEM image of a single particle and Ag nanoparticles size histogram, (c) HRTEM image of particle, showing the Ag nanoparticles on the surface of α-Fe_2O_3, (d) HRTEM image of Ag/Fe_2O_3 nanomaterial having a lattice plane with (110) indices of α-Fe_2O_3 and (111) and equivalent indices of Ag nanoparticle.

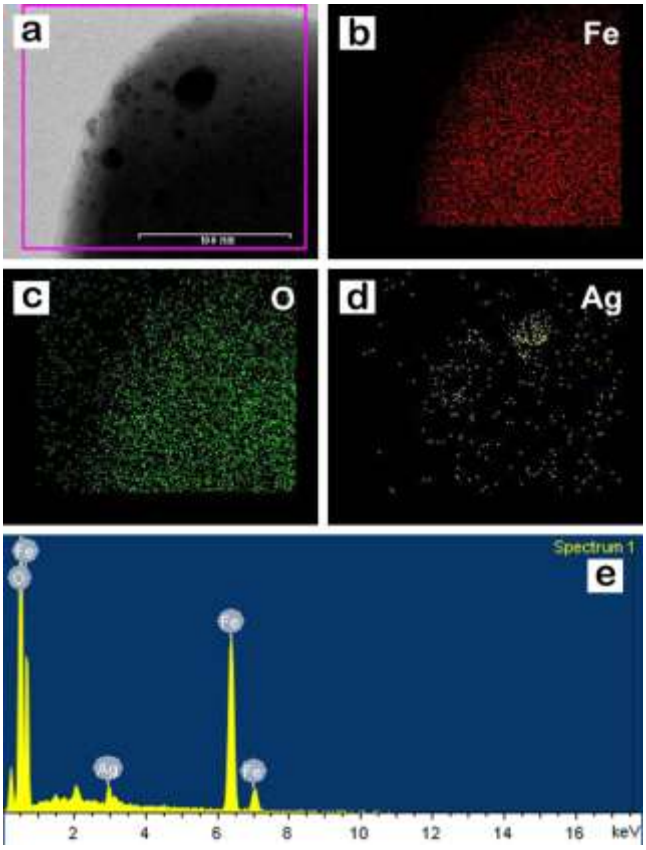

Fig. 4. (a) Dark-field STEM image of Ag/Fe_2O_3 nanomaterial and elemental mapping of (b) Fe, (c) O, and (d) Ag. The EDX spectrum of Ag/Fe_2O_3 nanomaterial is shown in (e).

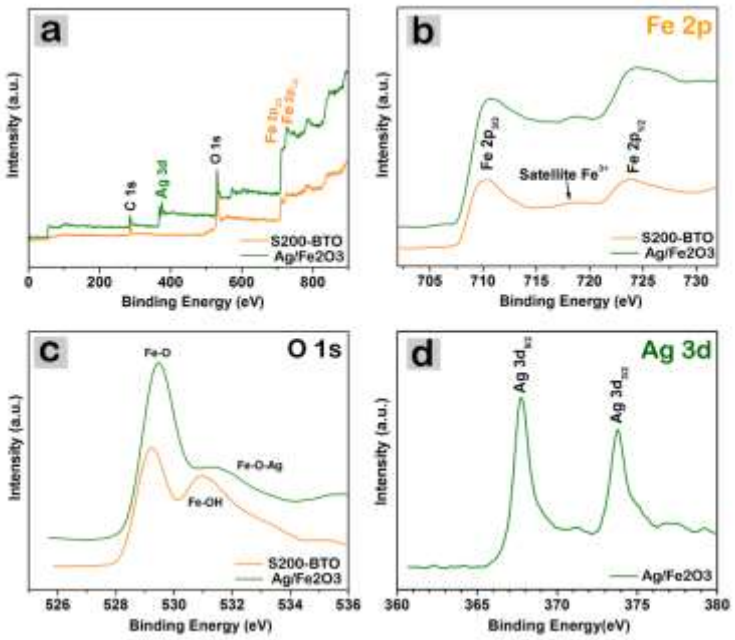

Fig. 5. XPS analysis of S200-BTO and Ag/Fe_2O_3 nanomaterials (a) survey XPS and High resolution XPS of (b) Fe 2p (c) O 1s (d) Ag 3d.

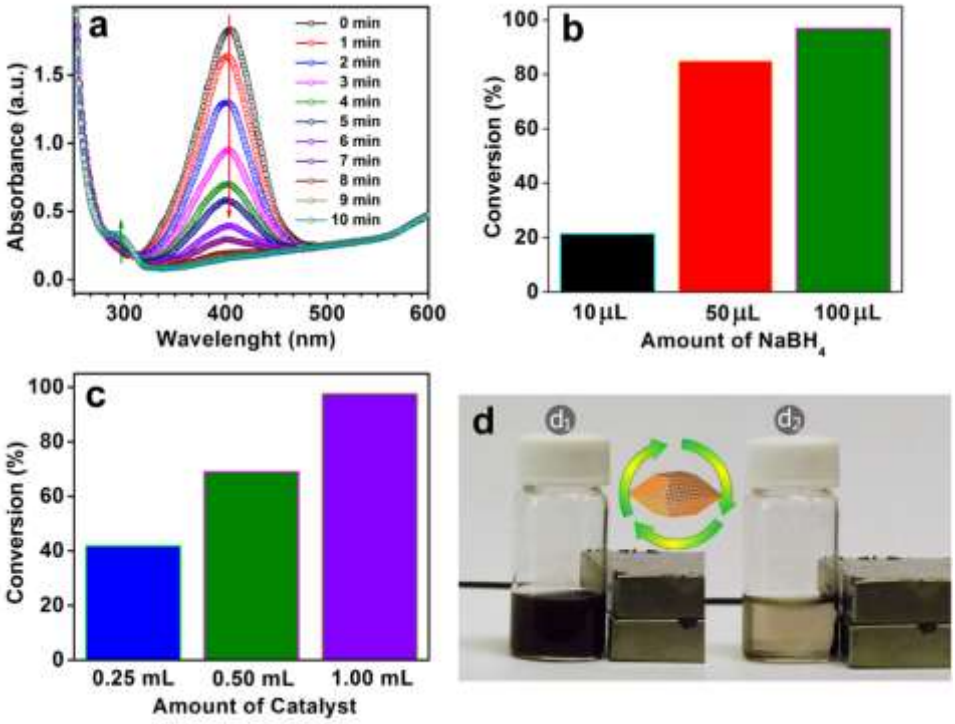

Fig. 6. (a) Kinetics study of hydrogenation reaction of 4-nitrophenol [Reaction condition: 2 ml of 0.1 mmol/L 4-nitrophenol, 500 µL of 1 mg/mL Ag/Fe_2O_3 nanocatalyst, and 200 µL of 10 mmol/L of $NaBH_4$], (b) Effect of $NaBH_4$ amount [Reaction condition: 2 ml of 0.1 mmol/L 4-nitrophenol, 500 µL of 1 mg/mL Ag/Fe_2O_3 nanocatalyst, and different amount of 10 mmol/L of $NaBH_4$ solution, and reaction carried out for 10 min], (c) Effect of catalyst amount [Reaction condition: 2 ml of 0.1 mmol/L 4-nitrophenol, different amount of 1 mg/mL Ag/Fe_2O_3 nanocatalyst, and 200 µL of 10 mmol/L of $NaBH_4$ solution, and reaction carried out for 5 min], and (d) Catalyst separate by external magnet.

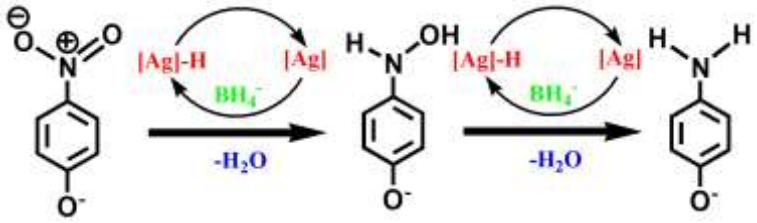

Fig. 7. Proposed reaction mechanism for Ag/Fe_2O_3catalyzed hydrogenation of nitroarene.

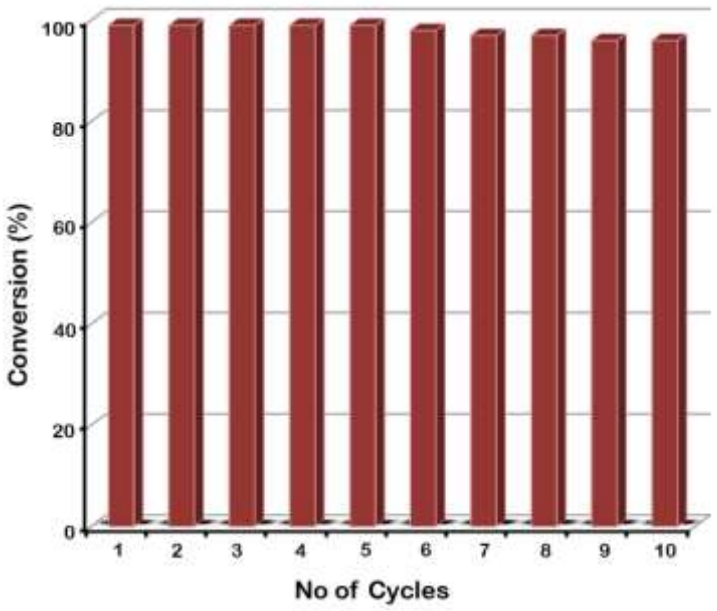

Fig. 8. Reusability of magnetic Ag/Fe_2O_3 nanocatalyst for hydrogenation of nitroarene in water.

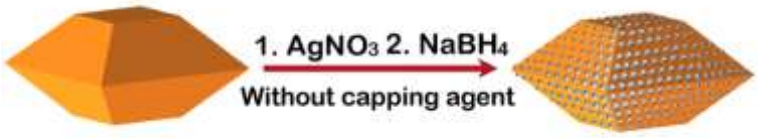

Scheme 1: Synthetic route of Ag nanocrystal decorated bitruncated-octahedron-shaped α-Fe_2O_3 nanocrystal via simple method.

Table 1. Optimization of Reaction Conditions on hydrogenation of 4-nitrophenol in the presence of Ag/Fe_2O_3 nanocatalyst in room temperature

Entry	Solvent	Hydrogen Source	Time (min)	Conversion (%)[a]
1	H_2O	$NaBH_4$	10	99
2[b]	H_2O	$NaBH_4$	10	6
3[c]	H_2O	$NaBH_4$	30	0
4	H_2O-Ethanol	$NaBH_4$	30	94
5	Ethanol	$NaBH_4$	30	8
6	THF	$NaBH_4$	30	0
7	DMF	$NaBH_4$	30	0
8	DCM	$NaBH_4$	30	0
9	Acetonitrile	$NaBH_4$	30	0

[a]Reaction condition: 2 ml of 0.1 mmol/L 4-nitrophenol, 500 µL of 1 mg/mL Ag/Fe_2O_3 nanocatalyst, and 200 µL of 10 mmol/L of $NaBH_4$; [b]Reaction carried out in absence of catalyst, [c]Reaction carried out with α-Fe_2O_3 (S200-BTO).

Table 2. Magnetic Ag/Fe_2O_3 nanocatalyst for hydrogenation of nitroarene in water in the presence of $NaBH_4$.

Entry	Reactant	Product	Time (min)	Yield (%)/ Selectivity (%)	TOF (h^{-1})
1	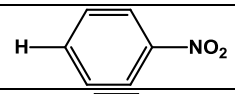	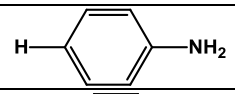	30	99/100	217.4
2	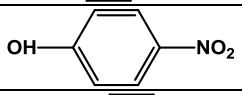	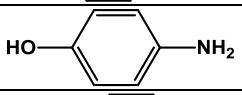	30	99.5/100	218.5
3	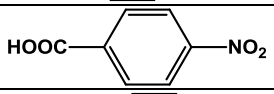	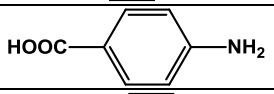	30	99.4/100	218.3
4	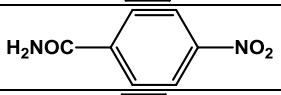	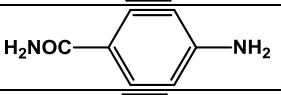	30	99/100	217.4
5	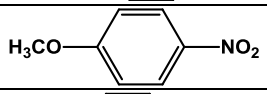	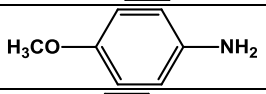	30	97.6/100	214.3
6	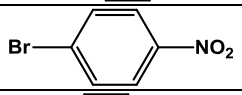	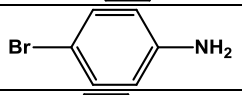	30	98/100	217.4
7	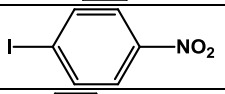	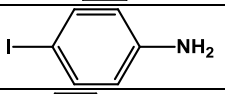	30	96/100	210.8
8	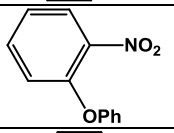	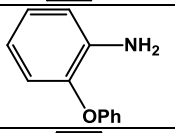	30	20.1/96	44.2
9[a]	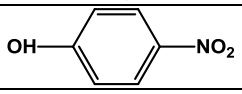	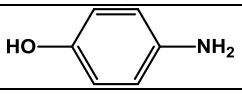	30	0	-

Reaction condition: nitroarenes substrate (0.2 mmol), Ag/Fe_2O_3 catalyst (5 mg, 1.821×10^{-6} mole Ag), $NaBH_4$ (2 mmol) and 10 mL of water. TOF (turnover number) = number of moles of substrate converted/number of moles of active site of the catalyst per hour, [a]Reaction carried out with α-Fe_2O_3 (S200-BTO).